

MICROSTRUCTURE AND CORROSION BEHAVIOUR OF THE BULK GLASSY $\text{Fe}_{68-x}\text{Co}_x\text{Zr}_{10}\text{Mo}_5\text{W}_2\text{B}_{15}$ ALLOYS

Grażyna Pawłowska¹, Piotr Pawlik², Henryk Bala¹ and Jerzy J. Wysłocki²

¹Institute of Chemistry, Częstochowa University of Technology, Al. AK 19, 42-200 Częstochowa, Poland

²Institute of Physics, Częstochowa University of Technology, Al. AK 19, 42-200 Częstochowa, Poland

Received: March 29, 2008

Abstract. Samples of $\text{Fe}_{68-x}\text{Co}_x\text{Zr}_{10}\text{Mo}_5\text{W}_2\text{B}_{15}$ ($x = 7, 9, 11$) bulk glassy alloys were produced in a form of 1 mm diameter rods by the suction-casting technique. XRD analysis revealed good glass forming abilities (GFA) of the investigated alloys. The corrosion characterization of the amorphous rods were performed in the absence and presence of chloride ions in sulphate test-solution. Analysis of potentiodynamic polarization curves indicates that the alloys undergo passivation in the applied media. For chloride containing solutions a distinct tendency to local corrosion has been observed. High Co containing alloy ($x=11$) exhibits clear worsening of corrosion behaviour as compared to the two other alloys.

1. INTRODUCTION

The Fe-based bulk glassy alloys attract the scientific interest due to a wide area of possible applications as well as relatively low processing costs. In this group of alloys especially attractive are $(\text{Fe,Co})_{68-x}\text{Zr}_{10}\text{Mo}_5\text{W}_2\text{B}_{15}$ -type alloys that reveal extremely good glass forming abilities (GFA). It was possible to process up to 6 mm diameter fully glassy rods for this type of alloys [1]. The investigation of Fe substitution by Co showed no significant change of their GFA [2]. Furthermore, large volume fractions of metalloids and refractory elements within the alloy compositions resulted in a reduction of the Curie temperature of the amorphous samples. Ferro- to paramagnetic transition was observed at around the room temperature for all investigated alloy compositions. Due to their very high mechanical hardness ($H_v \sim 1200$) and paramagnetic properties at room temperature the alloys might be utilized as structural materials for manufacturing of surgical blades. In the present paper a systematic study of the corrosion resis-

tance of $\text{Fe}_{68-x}\text{Co}_x\text{Zr}_{10}\text{Mo}_5\text{W}_2\text{B}_{15}$ ($x = 7, 9, 11$) alloys in various aggressive environments have been undertaken.

2. EXPERIMENTAL

The ingot samples of $\text{Fe}_{68-x}\text{Co}_x\text{Zr}_{10}\text{Mo}_5\text{W}_2\text{B}_{15}$ (where $x = 7, 9$ or 11) were produced by arc-melting the high purity elements under an Ar atmosphere. From the ingot samples 1 mm diameter rods were produced by suction-casting technique. The processing technique consists in the suction of liquid alloy into a copper die by applying a pressure difference between the two chambers integrated in the argon arc melting unit [3, 4]. In this way three kinds of rod samples were produced: sample "A" - for $x = 7$; sample "B" - for $x = 9$ and sample "C" - for $x = 11$ alloy, respectively.

For electrochemical tests, electrodes in the form of rotating discs, each of a working surface area of 0.02 cm^2 , were used. The geometrical area of the individual electrodes was determined with the accuracy $\pm 1\%$ on a metallographic microscope. The

Corresponding author: J. J. Wysłocki e-mail: wyslocki@mim.pcz.czyst.pl

Table 1. Tafel slopes (b_a and b_c) corrosion rates (i_{cor}) and polarization resistance (R_p) determined for the tested $Fe_{68-x}Co_xZr_{10}Mo_5W_2B_{15}$ alloys in 0.5 sulphate solution with $pH=0.3$. The corrosion rates have been calculated by extrapolation of Tafel segments and by linear polarization method.

| Sample | b_a [V] | b_c [V] | R_p [Ωcm^2] | i_{cor} [mAcm ⁻²] | |
|--------|-----------|-----------|-------------------------|---------------------------------|---------------------|
| | | | | Extrapolation | Linear polarisation |
| A | 0.12 | 0.12 | 400 | 0.04 | 0.06 |
| B | 0.12 | 0.12 | 300 | 0.06 | 0.09 |
| C | 0.06 | 0.12 | 70 | 0.2 | 0.2 |

Table 2. Effect of pH and chloride ions concentration on pitting potential (E_{pit} , V) of $Fe_{68-x}Co_xZr_{10}Mo_5W_2B_{15}$ materials.

| Sample | $pH=3,$ | $pH=3,$ | $pH=0,$ |
|--------|--------------------------|-------------------------|-----------------------|
| | [Cl ⁻]=0.05M | [Cl ⁻]=0.1M | [Cl ⁻]=1M |
| A | 1.3 | 0.67 | 0.20 |
| B | 1.3 | 0.54 | 0.19 |
| C | 0.79 | 0.53 | 0.20 |

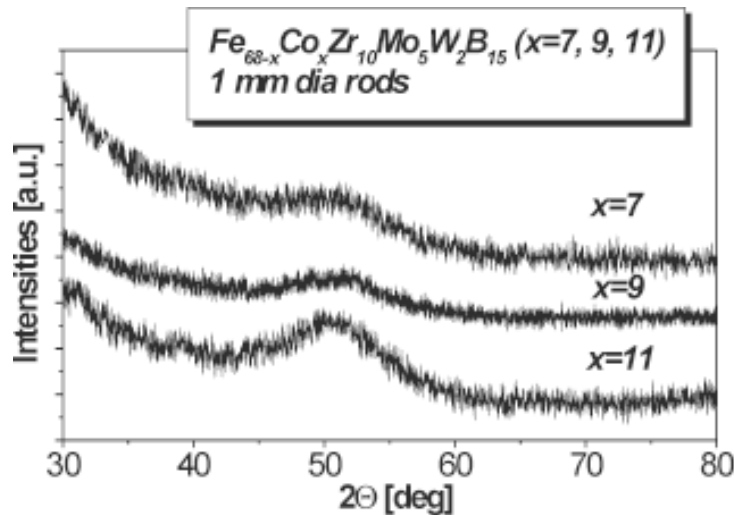


Fig. 1. The XRD patterns of $Fe_{68-x}Co_xZr_{10}Mo_5W_2B_{15}$ ($x=7, 9, 11$) 1 mm dia rods obtained by suction casting method.

discs were made by mounting particular specimen rods in metaplex caps using epoxy resin. Electrochemical tests were carried out in deaerated (Ar-saturated) solutions at a temperature of 25 °C, at a disc rotation speed of 16 rps and a scan rate of 10 mV/s, applying the potential shift from cathodic (-1.0 V) to anodic values (+2.0 V). CH Instruments CHI 680 potentiostat was used for potentiokinetic polarisation tests. The values of electrode poten-

tials were measured versus a saturated calomel electrode (SCE). The following polarisation measurements were carried out for the tested specimens: (i) potentiokinetic polarization curves in 0.5 M sulphate solutions with $pH = 0.3, 3.0,$ and $6.0,$ respectively and (ii) potentiokinetic polarization curves in solutions containing chloride ions: 1 M Cl⁻ ($pH = 0$) and acidified sulphate solutions ($pH = 3$) with an addition of 0.1 and 0.05 M Cl⁻.

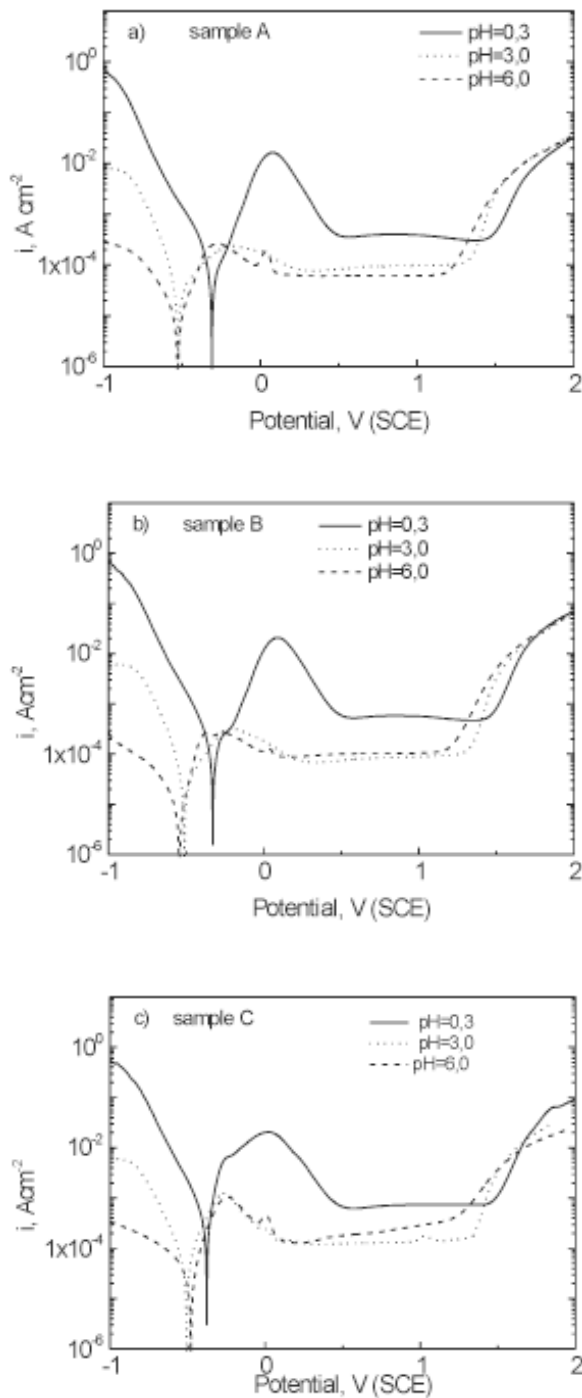


Fig. 2. Potentiokinetic polarisation curves of $Fe_{68-x}Co_xZr_{10}Mo_5W_2B_{15}$ materials in sulphate solutions $pH = 0.3, 3.0,$ and 6.0 (a) $x=7$; (b) $x=9$; (c) $x=11$.

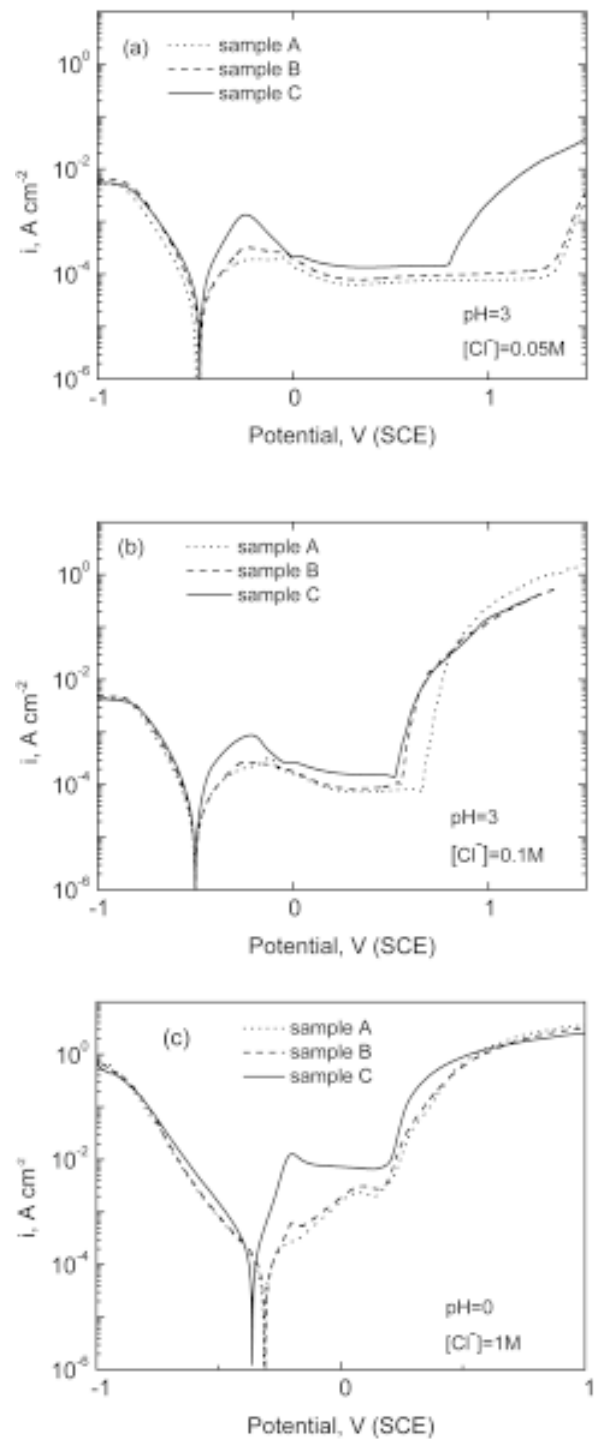


Fig. 3. Potentiokinetic polarisation curves of the tested $Fe_{68-x}Co_xZr_{10}Mo_5W_2B_{15}$ materials (samples A, B, and C) in acid sulphate solutions containing chloride ions.

3. RESULTS AND DISCUSSION

The X-ray diffraction pattern of the three investigated rod samples are shown in Fig. 1. For all al-

loy compositions an amorphous structure was exhibited with no sign of crystalline precipitates. The potentiokinetic polarization curves of the samples

tested in the acidified sulphate solutions with three different pH, are shown in Fig. 2. In all solutions tested, these bulk glassy alloys undergo effective passivation. The passivation ability of the investigated alloys in sulphate media, characterised by current density in the passive range and passivation potential, appeared to have been slightly better than these determined for pure iron [5]. The corrosion rates of the tested samples, determined by extrapolation of the rectilinear segments of potentiokinetic curves to E_{cor} polarization curve and by polarization resistance methods, are presented in Table 1. In the most acidic environment (pH = 0.3) the slope of the rectilinear segments in the cathodic region is approx. 0.12 V/decade. In the vicinity of the corrosion potential, the slope of the potentiokinetic curves clearly increases, which may result from preferential etching of more active constituents and surface development. The Tafel constants in the anodic region are equal to $b_a = 0.12$ V/decade for specimens A and B and $b_a = 0.06$ V/decade for specimen C. The lower slope of the Tafel segment for specimen C indicates a different mechanism of anodic dissolution of the material containing 11 at.% Co. Similar tendency for change in the corrosion mechanism is observed for potentials slightly more noble than E_{cor} also for the specimen containing 9 at.% Co. Thus, the increase in Co content favours the process of the alloy active dissolution, which can be ascribed to a much higher value of Co^{2+}/Co exchange current compared to Fe^{2+}/Fe . As it is known, cobalt is thermodynamically more noble than iron: $E_{\text{Co}^{2+}/\text{Co}}^0 = -0.28$ V whereas $E_{\text{Fe}^{2+}/\text{Fe}}^0 = -0.44$ V. Thus, in case the exchange currents were comparable for both metals, iron would dissolve first. The extrapolation of the rectilinear anodic and cathodic segments of polarisation curves allows to determine corrosion rate and corrosion potential (i_{cor} and E_{cor} , respectively). In the case of specimen B due to the "hump" occurring in the anodic curve (Fig. 2b), the extrapolation of only cathodic segment to E_{cor} was applied. The corrosion rates determined by extrapolation are in good agreement with those obtained by the linear polarization method (Table 1). The corrosion rates of specimens A and B are generally much lower than those found for pure iron in the same environment ($i_{\text{cor,Fe}} \approx 0.1$ mAcm⁻² for 0.5M SO_4^{2-} solution with pH = 0.3) [6]. The specimen C (containing 11 at.% Co) corrodes in the acidic sulphate environment 3-4 times faster than samples A and B. The effect of acidity on corrosion behaviour of

the tested samples is presented in Fig. 2. Transition from the strongly acid environment (pH = 0.3) to the acidified environment (pH = 3.0) results in a distinct drop of anodic current densities in passive range and a shift in corrosion potential towards more negative values. On the other hand, the further increase in pH does not practically cause any noticeable changes in anodic region. In cathodic range, distinct decrease of cathodic currents with pH increase is visible and for pH = 3 and 6 the cathodic process becomes diffusion controlled. The thermodynamic susceptibility of $\text{Fe}_{68-x}\text{Co}_x\text{Zr}_{10}\text{Mo}_5\text{W}_2\text{B}_{15}$ materials to local corrosion has been characterized in the present study by determination of pitting potential (E_{pit}) in solutions containing chloride ions. The pit nucleation potentials were determined for strong (pH = 0) and medium acid solutions (pH = 3) with Cl^- ions concentration being 0.05, 0.1, and 1M. In Fig. 3 the corresponding polarisation curves are presented. As it results from Figs. 3a and 3b, for medium acid solution an increase in Co content leads to a decrease of E_{pit} in both chloride containing solutions. However, breakdown of the passive layer at a lower concentration of chloride ions ($[\text{Cl}^-] = 0.05$ M) occurs only in the high-cobalt alloy. For strong acid solution containing 1M Cl^- (Fig. 3c) the passive film breakdown potential is virtually identical for all specimens (compare Table 2). As it can be seen from Figs. 3a-3c, the decrease in E_{pit} value, which describes increasing tendency to local corrosion, is accompanied by a distinct increase in the anodic current in passive region. This way, worsening of passive properties of the alloy with Co content increase significantly favors local corrosion attack by chloride ions.

4. CONCLUSIONS

The $\text{Fe}_{68-x}\text{Co}_x\text{Zr}_{10}\text{Mo}_5\text{W}_2\text{B}_{15}$ bulk glassy alloys effectively passivate in sulphate environments unless the solution is strongly acidic. The corrosion rate in an acidified sulphate environment increases with increasing cobalt content in the $\text{Fe}_{68-x}\text{Co}_x\text{Zr}_{10}\text{Mo}_5\text{W}_2\text{B}_{15}$ alloys. The 11 at.% of Co alloy corrodes according to a different mechanism compared to specimens with a lower Co content which is manifested by distinct change of anodic Tafel slope in sulphate acid medium. Increase in Co content in $\text{Fe}_{68-x}\text{Co}_x\text{Zr}_{10}\text{Mo}_5\text{W}_2\text{B}_{15}$ alloys is detrimental from their pitting corrosion point of view.

ACKNOWLEDGEMENTS

Work supported by the Polish Ministry of Scientific Research and High Education (grant: 3T08A 046 27)

REFERENCES

- [1] A. Inoue // *Acta Mater.* **48** (2000) 279.
- [2] P. Pawlik and H.A. Davies // *J. Non-Cryst. Sol.* **329** (2003) 17.
- [3] G. Pawłowska, H. Bala and P. Pawlik // *Ochr. przed Korozją 11s/A* (2005) 88, In Polish.
- [4] P. Pawlik, M. Nabiałek, E. Żak, J. Zbroszczyk, J. J. Wysocki, J. Olszewski and K. Pawlik // *Arch. Mater. Sci.* **25** (2004) 177.
- [5] K. Giza, H. Bala, L. Adamczyk, K. Gęsiarz, I. Przerada, E. Owczarek and B. Rożdżyńska-Kielbik // *Ochr. przed Korozją 11s/A* (2005) 39, In Polish.
- [6] H. Bala // *Electrochim. Acta* **29** (1984) 119.